Isomerization of an η^3-Allyl to an (*E*)-1-Propenyl in $(C_5Me_5)(C_5Me_4CH_2)TiC_3H_5$: Mechanism, Kinetics, and Thermodynamics

Peter H. P. Brinkmann,[†] Gerrit A. Luinstra,*[,†] and Alejandro Saenz[‡]

Contribution from the Inorganic Chemistry and Physical Chemistry Sections, Department of Chemistry, University of Konstanz, Fach M738 and M722, D-78457 Konstanz, Germany

Received August 14, 1997

Abstract: The isomerization of Cp*FvTi(η^3-C_3H_5) (**1**) to Cp*FvTi((*E*)-CH═CHMe) (**5**) proceeds through four intermediates, Cp*$_2$Ti(η^2-allene) (**2**), two geometrical isomers of Cp*FvTiCMe═CH_2 (**3a**,**b**), and Cp*$_2$Ti(η^2-propyne) (**4**) (Cp*, C_5Me_5; Fv, $C_5Me_4CH_2$). The process was monitored at four temperatures between 10 and 40 °C starting from **1** or the mixture **3a**,**b**. The time-dependent concentration profiles of all compounds were simulated with a mathematical model of 10 rate constants. The model is based on the assumption that the isomerization proceeds through reversible first-order reaction steps in the sequence **1** ⇌ **2** ⇌ **3a** ⇌ **3b** ⇌ **4** ⇌ **5**. Equilibrium constants yield Gibbs free energy differences between the complexes ranging from 0 to −8 kJ/mol. The activation enthalpies for the forward reactions lie between 75 and 102 kJ/mol and between 74 and 111 kJ/mol for the reverse reactions. The entropy of activation is negative for the forward and reverse reactions between **1** and **2** and between **4** and **5** and positive for transitions involving the sterically congested isomers **3a**,**b**, except for the rotation of the isopropenyl group in **3a**.

Introduction

In a recent paper, we described the synthesis and the C−H activation processes in Cp*FvTiR compounds (Cp*, η^5-C_5Me_5; Fv, $C_5Me_4CH_2$; R = Et, CH_2Ph, CH_2SiMe_3, CH_2CMe_3).[1] The tetramethyl fulvene (Fv) ligand is involved in the reactivity of these compounds: in the more interesting mode, the exocyclic methylene entity takes up an H^- (hydride) to form a Cp* ligand.[2] It was noted that the allyl derivative Cp*FvTiC_3H_5 (**1**) isomerizes to Cp*FvTi((*E*)-CH═CHMe) (**5**) (eq 1). We wanted to

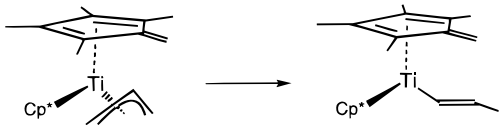

(1)

use this isomerization in combination with a transmetalation step to catalytically transform metal allyl into metal *trans*-1-propenyl compounds: **1** → **5**, $L_nM(\eta^3$-allyl) + **5** → L_nM((*E*)-CH═CHMe) + **1**, etc.[3] However, it was found that neither Cp*FvTiCl nor **1** catalyzes the conversion of, e.g., BrMgAllyl to (*E*)-BrMgCH═CHMe.[4] We decided to take a closer look at the isomerization **1** → **5** and to gain insight into the kinetics and the thermodynamics of the process to possibly find a reason for the absence of the catalysis. Four intermediates were observed and identified by ^{1}H NMR spectroscopy. They are interconnected to each other and to **1** and **5** through reversible elementary reaction steps—a hydrogen transfer or a rotation. The activation energies of all reactions and their inverses were obtained from a kinetic analysis. This represented quite a challenge due to the size of the reaction system. It is, however, seldom that so many intermediates can be observed in such a cascade of reactions.[5] It thereby forms a textbook example of metal-mediated catalysis, wherein the random orientation in the allyl group is selectively transformed into the regiospecific (*E*)-propenyl entity through all obvious reaction intermediates and is relevant to the thermodynamic stability and kinetics of metal-bound C_3 fragments. The outcome of the in-depth kinetic analysis of the isomerization of eq 1 reveals a very smooth reaction pathway for the reaction from **1** to **5**. The aforementioned reaction mode of the fulvene group is of crucial importance for this process, acting next to the metal as a second reactive site. The importance of the relative orientation of Fv and $C_3H_{4/5}$ fragments is not very different compared to that found in enzyme catalysis.

Experimental Section

All operations were performed in an inert atmosphere with rigorous exclusion of oxygen and moisture using Schlenk, vacuum line, or

[†] Inorganic Chemistry, Fach M738.

[‡] Physical Chemistry, Fach M722.

(1) Luinstra, G. A.; Brinkmann, P. H. P.; Teuben, J. H. *J. Organomet. Chem.* **1997**, *532*, 125.

(2) If this occurs intermolecularly through reaction of an alkane with the fulvene entity, a metal alkyl is produced. This has been considered a key step toward the functionalization of alkanes. It is the reverse of the formation of tetramethyl fulvenes from coordinating permethyl Cp by methyl group hydrogen abstraction, a common feature of the thermolysis of early transition metal and lanthanide permethylmetallocene alkyls; see references cited in ref 1.

(3) As in the alkylation of olefins with Grignards, catalyzed by Cp_2Zr^{II}; see, e.g.: Hoveyda, A. H.; Morken, J. P. *Angew. Chem.* **1996**, *108*, 1378. Also, from a "commercial" point of view, this is an interesting reaction: Aldrich prices for allyl bromide ≈ $0.10/g and (*E*)-BrCH═CHMe ≈ $30/g would make this an interesting conversion.

(4) Reaction of Cp*FvTiCl with an excess of allylMgBr resulted—after formation of **1**—in a slow reduction to Cp*FvTi, and, moreover, formation of **1** from **5** and allyl Grignard reagent does not occur. With $(allyl)_2Zn$, deposition of Zn occurs before substitution has taken place, and Cp*FvTi-(*E*)-CH═CHMe is decomposed by $(allyl)_3B$. (a) Thiele, K. H.; Zdunneck, R. *J. Organomet. Chem.* **1965**, *4*, 10. (b) Topchiev, A. V.; Paushjin, M. Y.; Prokhorova, A. A. *Dokl. Akad. Nauk. SSSR* **1959**, *129*, 598.

(5) Takahashi, T.; Nishihara, Y.; Sun, W.-H.; Fischer, R.; Nakajima, K. *Organometallics* **1997**, *10*, 2216.

S0002-7863(97)02867-9 CCC: $15.00
Published on Web 03/18/1998

glovebox techniques. Solvents were thoroughly dried (ether and THF over Na/benzophenone, pentane over Na/K alloy, toluene over Na) and distilled prior to use. Benzene-d_6 was vacuum transferred from Na/K alloy. IR spectra were recorded on a Mattson Galaxy spectrometer as Nujol mulls between KBr disks. NMR spectra were recorded on Bruker WM250, AC250, DXR 600 Avance or JEOL FX-90Q, JNM GX400 spectrometers. Chemical shifts are reported in ppm and referenced to residual protons in deuterated solvents (benzene-d_6, $\delta = 7.15$ ppm) for ^{1}H NMR and to characteristic multiplets for ^{13}C NMR (benzene-d_6, $\delta = 127.98$ ppm). Elemental analyses were carried out at the Micro-Analytical Department of the University of Konstanz. Cp*FvTiC$_3$H$_5$ was prepared as reported previously.[1] LiCMe=CH$_2$ was prepared from Li and BrCMe=CH$_2$ in ether, and BrMgCMe=CH$_2$ and (*E*)-BrMgCH=CHMe were prepared from Mg and the bromoalkenyl compounds in THF, according to standard laboratory procedures.

Cp*FvTi(2-propenyl) (3a,b). To a solution of Cp*FvTiCl (282 mg, 0.8 mmol) in 5 mL of ether at −40 °C was added 2.2 mL of a 0.37 M solution of LiCMe=CH$_2$ (0.8 mmol) in ether. The mixture was allowed to warm to 0 °C. The solvent was exchanged for pentane, and after filtration (at 0 °C), concentration, and crystallization at −80 °C, 84 mg (0.23 mmol, 29%) of a blue-green solid was collected. The compound is extremely soluble in pentane. IR (cm^{-1}): 2720 (w), 1655 (vw), 1665 (vw), 1560 (w), 1285 (w), 1165 (m), 1065 (w), 1025 (s), 980 (w), 870 (m), 830 (m), 745 (w), 610 (w), 570 (w), 545 (w), 455 (m). Anal. Calcd for C$_{23}$H$_{34}$Ti: C, 77.07: H, 9.56. Found: C, 77.29; H, 9.64.

The compound may also be prepared from BrMgCMe=CH$_2$ and Cp*FvTiCl in a similar way, but the reaction takes about 24 h at 0 °C.

(*E*)-Cp*FvTi(CH=CHMe) (5). Cp*FvTiCl (290 mg, 0.82 mmol) was dissolved in 6 mL of THF, and 2.1 mL of a 0.4 N (*E*)-BrMgCH=CHMe (0.84 mmol) solution in THF was added. The mixture was stirred for 4 h, after which the THF was exchanged for pentane. After filtration and crystallization at −80 °C, 101 mg (0.28 mmol, 34%) of green-blue crystals were isolated. IR (cm^{-1}): 2720 (w), 1645 (w), 1574 (m), 1295 (s, br), 1170 (m), 1025 (s), 980 (m), 850 (w), 825 (s), 745 (m), 680 (w), 570 (w), 550 (w), 490 (s), 410 (s). Anal. Calcd for C$_{23}$H$_{34}$Ti: C, 77.07: H, 9.56. Found: C, 76.85; H, 9.24.

Synthesis of 5 from 1 or 3a,b. Cp*FvTi(C$_3$H$_5$) (254 mg) was dissolved in 10 mL of ether. The mixture was refluxed for 5 h, after which the volatiles were removed in a vacuum. The ^{1}H NMR spectrum of the resulting sticky material revealed that **5** had been formed almost quantitatively. The residue was dissolved in 2 mL of pentane, and subsequent cooling to −80 °C yielded 83 mg (33%)[1] of **5** as dark green-blue crystals. The mixture **3a**,**b** thermolyses at room temperature in the solid state quantitatively to **5**.

Kinetic Measurements. A 4−10-mg portion of the fulvene compound **1** or **3a**,**b** was dissolved in 0.5 mL of benzene-d_6 and then quickly transferred into an NMR tube, which was subsequently cooled in liquid nitrogen and flame-sealed. The probe head of a 400-MHz NMR spectrometer was thermostated at the desired temperature, and then the sample was thawed and instantly inserted. ^{1}H NMR spectra were recorded at preset intervals. The concentrations of the compounds were taken from the integrated intensities of the "olefinic" resonances between 3.9 and 6.95 ppm, with the sum of the values serving as the normalization factors. Since the reaction already started during sample preparation, thermostating, and shimming, initial conditions are not very precisely defined, and hence they are approximated as described below.

Mathematical Analysis of the Model. The numerical analysis was performed using a homemade FORTRAN program (containing NAG and IMSL library routines). One computation takes about 3−6 min if performed on a DECstation 5000/125. Time profiles are calculated from rate constants as variables by solving a matrix−eigenvalue problem (see Appendix)[6] and then compared with experimental data. The optimum values for the rate constants were determined by minimizing the quantity

$$\chi^2 = \sum_i \sum_j \frac{[c_j^{\mathrm{exp}}(t_i) - c_j^{\mathrm{calc}}(t_i)]^2}{|c_j^{\mathrm{exp}}(t_i)|}$$

where $c_j^{\mathrm{exp}}(t_i)$ is the measured concentration of compound j (j = **1**, **2**, **3a**, **3b**, **4**, **5**) at time t_i, and $c_j^{\mathrm{calc}}(t_i)$ is the corresponding concentration calculated for a given set of rate constants. The minimum was obtained with the aid of the IMSL ZXNWD global-minimum finder with constraints (100−200 start vectors). For the reactions starting from the pure compound **1**, the differential equations were solved for the initial conditions $c_1(t = 0) = 1$ and $c_j(t = 0) = 0$ (for $j \neq 1$), while 10 rate constants and one time offset were used as fit parameters. Starting from the mixture **3a**,**b**, only 10 rate constants were used as fit parameters, and all experimental data were used to define the boundary conditions for solving the differential equations (by virtue of a linear least-squares fit).

Rate constants were limited to values within preset intervals, which were contracted in subsequent computations to reduce computation times. Only reactions between consecutively numbered compounds were allowed, as defined in Scheme 1. Satisfactory to good fits of the experimental data were obtained by this procedure. From manually varying the optimized rate constants, it was estimated through a visual comparison of the calculated time profiles and the experimental data that the final rate constants have an error that is smaller than 30% of the values given. It has to be considered, though, that only local minima can be obtained that need not be global. It is, nevertheless, remarkable that it was possible to consistently determine the comparatively large number of fit parameters from the experimental data with a minimum number of rate constants.

Results and Discussion

Identification of the Reaction Intermediates. A complex mixture of compounds soon forms when a solution of **1** is heated, as is evident from the ^{1}H NMR signals. This mixture of compounds was analyzed by 2D NMR techniques, leading to the identification of five compounds.[7] They account for all of the observed NMR signals (Table 1).

The allyl group in the starting complex, Cp*FvTi(C$_3$H$_5$) (**1**), is η^3-coordinated with rapidly equilibrating endo and exo positions. In the ^{1}H NMR spectrum, a characteristic quintet is found with a ^3J(HH) of 12.2 Hz for the proton on the central carbon and one doublet with the same coupling constant and a relative intensity of four protons. No NOEs were observed between the allyl and the Cp* or Fv ligands.[7]

The first new compound to be identified was the allene adduct of permethyl titanocene, Cp*$_2$Ti(CH$_2$=C=CH$_2$) (**2**). It shows a singlet in the ^{1}H NMR at 1.68 ppm for the Cp* methyl protons. This is the same position as found for the ethene adduct, Cp*$_2$-Ti(CH$_2$=CH$_2$).[8] The allene fragment is η^2-bonded and is not fluctional. It shows the splitting pattern of an ABC$_2$ spin system, comparable to that of Cp*$_2$TaH(CH$_2$=C=CHMe)[9] and Cp$_2$Ti-(CH$_2$=C=CH$_2$)PMe$_3$.[10] In the ^{13}C NMR spectrum, signals for the coordinated allene fragment were observed at 87.3, 120, and 104 ppm. The large high-field shift of the latter was also found in the ethene adduct (104 ppm).[8] Strong NOE cross signals are observed among the protons in the coordinated allene, but not between the C$_3$ entity and the Cp* or Fv group.

(6) See: Bittrich, H.-J.; Haberland, D.; Just, G. *Methoden chemisch kinetischer Berechnungen*; VEB: Leipzig, Germany, 1986; Chapter 4.

(7) At those times during the thermolysis when the concentration of a certain intermediate was such that the NMR signals were conveniently observable, the mixture was cooled and analyzed by correlation spectroscopy to give the connectivity and spatial arrangement in the intermediates. The reaction was also monitored by IR spectroscopy (in benzene-d_6). However, no characteristic features were found that allow rate determinations in the time-dependent spectra.

(8) Cohen, S. A.; Auburn, P. R.; Bercaw, J. E. *J. Am. Chem. Soc.* **1983**, *105*, 1136.

(9) Gibson, V. C.; Parkin, G.; Bercaw, J. E. *Organometallics* **1991**, *10*, 220.

(10) Binger, P. *Chem. Ber.* **1994**, *127*, 39.

Scheme 1

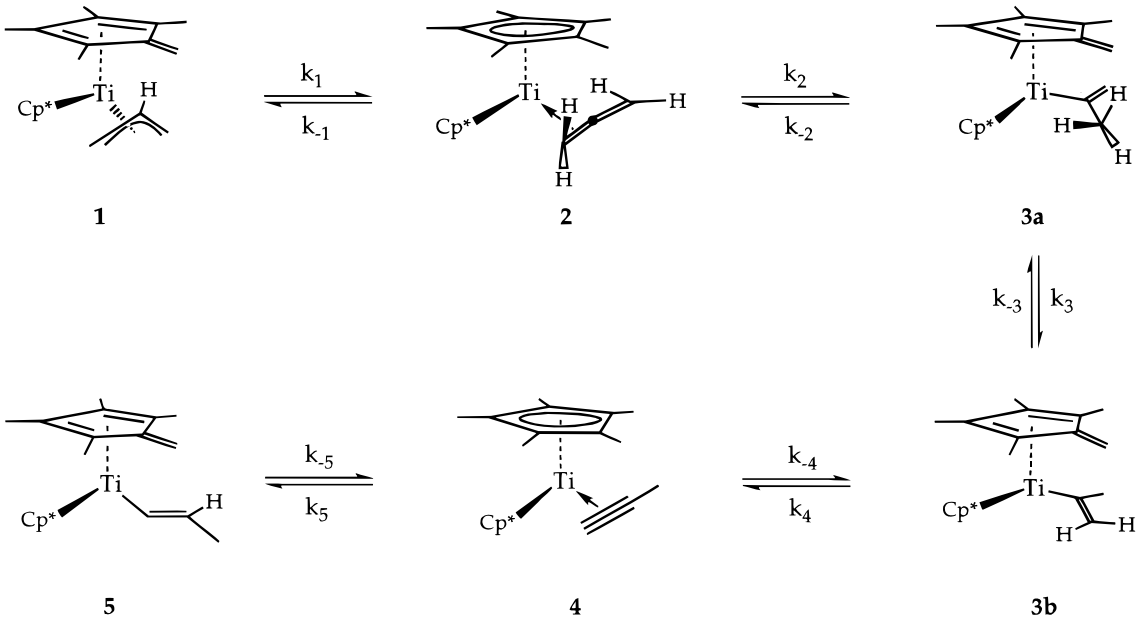

Table 1. Proton NMR Data of Cp*FvTiR in Benzene-d_6 at 10 °C

compound	assign-ment	δ, ppm	int (H)	m	J(HH), Hz
Cp*$_2$Ti(CH$_2$=C=CH$_2$) (**2**)	Cp*	1.68	15	s	
	=CH$_2$	2.45	2	t	3.4
	=CH$_2$	3.86	1	dt	2.4, 3.4
		5.8	1	dt	2.4, 3.4
Cp*FvTi(2-propenyl) (**3a**)	Cp*	1.77	15	s	
	C$_5$Me$_4$	1.26	3	s	
		1.41	3	s	
		1.68	3	s	
		2.02	3	s	
	=CH$_2$	1.36	1	d	4.5
		1.68	1	d	4.5
	C*Me*=CH$_2$	1.15	3	ps t	1.3
	CMe=C*H*$_2$	3.45	1	dq	3.1, 1.2
	CMe=C*H*$_2$	5.34	1	dq	3.1, 1.4
Cp*FvTi(2-propenyl) (**3b**)	Cp*	1.77	15	s	
	C$_5$Me$_4$	1.21	3	s	
		1.43	3	s	
		1.69	3	s	
		2.06	3	s	
	=CH$_2$	1.41	1	d	4.3
		1.93	1	d	4.3
	C*Me*=CH$_2$	1.16	3	ps t	~1.4
	CMe=C*H*$_2$	3.67	1	dq	2.8, 1.1
	CMe=C*H*$_2$	5.18	1	dq	2.8, 1.4
Cp*$_2$Ti(HC≡CMe) (**4**)	Cp*	1.7	15	s	
	HC≡C*Me*	1.77	3	d	2.1
	*H*C≡CMe	6.83	1	q	2.1

Further identified were two isomers of a compound with a connectivity as in Cp*FvTiCMe=CH$_2$ (**3a**,**b**). The 2-propylene unit gives rise to an ABX$_3$ spin system. The olefinic resonances are observed at 3.44 and 5.34 ppm for isomer **3a** and at 3.65 and 5.15 ppm for isomer **3b**. Based on the NOESY spectrum, the high-field shifts are assigned to the positions pointing toward the metal (proximal, Figure 1). The isopropenyl methyl group of **3a** and **3b** resonates at 1.15 and 1.16 ppm, respectively (at 10 °C). These shifts are somewhat dependent on the temperature. Also, small differences in shifts were observed for the methyl groups of the fulvene in **3a** and **3b**, and the same shift was observed for the Cp* ligand. The two possible geometric isomers are depicted in Figure 1. They differ only in the relative orientation of the vinyl groups of the 2-propylene group and

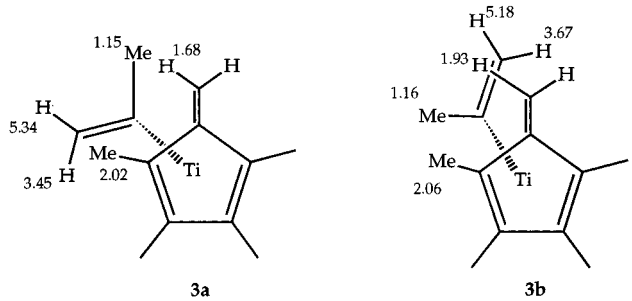

Figure 1. Two isomers of Cp*FvTiC(Me)=CH$_2$ (**3a**,**b**) with their ^{1}H NMR signals.

the exocyclic methylene of the fulvene ligand. It is assumed that rotation around the Ti−C bond is hindered. Restricted rotation is not uncommon in sterically congested Cp*$_2$Ti^{IV} compounds.[11] The assignment of the signals to a mixture **3a**,**b** was additionally confirmed by the independent synthesis of these rotamers from Cp*FvTiCl and LiCMe=CH$_2$ (and from BrMg-CMe=CH$_2$; a 1:1 mixture is formed in both cases).

We have assigned one set of signals to the first structure in Figure 1 (**3a**) and the other set to the second structure (**3b**). This choice is based on observations made during the thermolysis (vide infra) and cannot be proven conclusively. The assignment, however, is in accordance with the following. By examination of the structures in Figure 1, the methyl group of the C$_3$ fragment in **3a** seems closer to the fulvene methylene group, whereas in **3b** the methylene group would have the smallest distance. A NOESY spectrum of a mixture of **3a**,**b**, however, was not particularly informative: as in **1** and **2**, no strong cross relaxation between the C$_3$ and Fv-bound protons is present. In both **3a** and **3b**, cross relaxation between the C−*H* resonance of the exocyclic methylene of the fulvene and the proximal C$_3$ vinylic protons is observed (3.45 to 1.68 and 3.67 to 1.93 ppm; it was previously inferred from ^{1}H NMR shifts and NOESY cross signals in a number of Cp*FvTiR derivatives[1] that the fulvene methyl resonating around 2.01-(30) ppm and the methylene proton at 1.92(30) ppm are most likely in the proximity of group R), but this does not allow a

(11) Luinstra G. A.; Vogelzang, J.; Teuben, J. H. *Organometallics* **1992**, *11*, 2273.

structure assignment. The signal at 5.18 ppm of **3b** (the distal vinylic C−*H* of the C_3H_5 entity) has a small cross-peak to the fulvene methyl resonating at 2.06 ppm. In **3a**, a stronger signal at 5.43 to 2.02 ppm and a very weak one to 1.68 (=CH_2 of the fulvene) is found. Likewise, the cross relaxation between Cp* and the distal vinylic proton in **3a** seems stronger than the corresponding signal in **3b**. These observations, indeed, are consistent with our assignment. Other possible diagnostic interactions, such as those between the C_3 methyl groups and the fulvene methyl groups, could not be resolved in the 2D spectrum, and those between the exocyclic methylene protons are obscured by strong diagonal interactions. Hence, no compelling evidence could be obtained for the structure of either isomer.

A fourth compound is characterized as the propyne adduct of permethyl titanocene, Cp*$_2$Ti(η^2-HC≡CMe) (**4**). The acetylenic proton is found at low field (6.82 ppm) as a quartet, coupled to the doublet at 1.77 ppm of the methyl group. It is unlikely that the compound is the vinylidene isomer, Cp*$_2$-Ti=C=CHMe, which would exhibit the same splitting pattern. The small coupling constant of J(HH) = 2.1 Hz is not consistent with this: a larger coupling constant of J(HH) = 6.9 Hz was found in, e.g., Cp*$_2$Ta(H)=C=CHMe.[9] In addition, permethyltitanocene vinylidenes are very reactive and undergo fast rearrangements; Cp*$_2$Ti=C=CH_2 in the thermolysis of Cp*$_2$-Ti(Me)CH=CH_2 (methane extrusion) was too unstable to be observed, and not even phosphine adducts of the complex were detected.[12]

Toward the end of the thermolysis, a fifth compound is formed, characterized as (*E*)-Cp*FvTiCH=CHMe (**5**). It again shows an ABX_3 spin system, with a vinylic J(HH) of 17.4 Hz, indicative of a trans arrangement of the two protons. NOE cross signals between the 1-propenyl methyl group to either Cp* or fulvene were not observed, but the vinylic protons show a cross relaxation to each other. The identity of this compound was confirmed by its synthesis through the reaction of Cp*FvTiCl with (*E*)-BrMgCH=CHMe.

Order of Appearance of the Reaction Intermediates and Reversibility of All Steps. In the first stage of the isomerization starting from **1**, the allene adduct **2** is the only new feature. Next, the concentration of **3a**, **3b**, and **4** becomes significant, and, toward completion, product **5** is the predominant species. Concentration profiles of the equilibration of **1** → **5** are shown in Figure 2A. The decomposition of **1** follows an exponential rate law. The compounds **2**, **3a**, **3b**, **4** behave like typical reaction intermediates:[13] their concentrations increase and subsequently decrease with time. The concentration of **2** is the first to increase and to reach its maximum. Consequently, it is likely that **2** is the first intermediate. The place of the other compounds in the isomerization process is less clear from this experiment.

More information on the isomerization process was obtained from the thermolysis of the 1:1 mixture **3a**,**b**. During its decomposition, all the compounds **1**−**5** become observable at some stage of the reaction (by ^{1}H NMR spectroscopy, Figure 2B), demonstrating that at least **1**, **2**, and **3a**,**b** are interconnected through reversible reactions. In the very early stage of this reaction, the concentration of **3b** decreases by the same rate as **4** increases, and the increase in the concentration of **2** correlates with the decrease in **3a**. This indicates that **4** is formed from **3b**, and **2** is formed from **3a**. It is from this observation that **3a** and **3b** are assigned their respective structures.

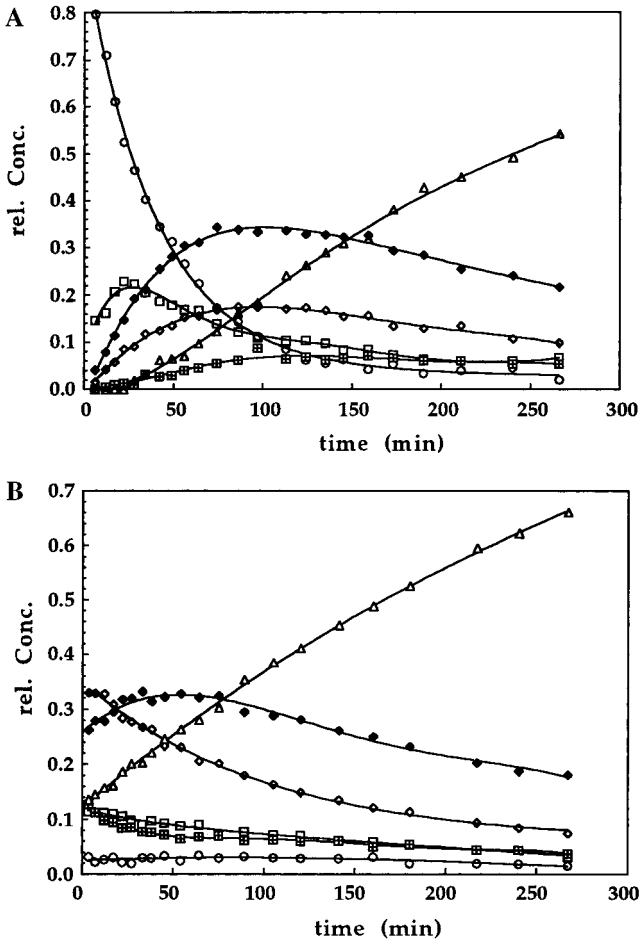

Figure 2. Concentration profiles of the equilibration at 20 °C of **1** to **5**, starting from **1** (A) and **3a**,**b** (B), with interpolated curves. ○, **1**; □, **2**; ◇, **3a**; ⊞, **3b**; ◆, **4**; and △, **5**.

Table 2. Temperature-Dependent Equilibrium Constants of **4** ⇌ **5**

temp (°C)	K	temp (°C)	K
20.0	0.0305	60.0	0.0483
30.0	0.0354	70.0	0.0526
40.0	0.0396	80.0	0.0588
50.0	0.0445		

The complex ^{1}H NMR spectrum that arises from the reaction of (Cp*$_2$TiN$_2$)$_2$(μ-N$_2$)[14] and propyne in benzene-d_6 provides evidence for the formation of **4**. After some time, the resonances of **3a**,**b** and **5** were also detected in the solution. This demonstrates that **3a**,**b** and **4** are also part of an equilibrium system. The final product **5**, obtained from the chloride substitution in Cp*FvTiCl, is stable at room temperature; a close examination of the NMR spectra revealed the presence of small amounts of the propyne adduct **4**. This indicates that the last step of the isomerization leading to **5** is also reversible. The equilibrium constants for **4** ⇌ **5** were determined by NMR between 20 and 70 °C, leading to ΔH^0 = 9.1(3) kJ/mol and ΔS^0 = 2(1) J/(mol·K) (Table 2).

Tentative Isomerization Pathway. A pathway for the isomerization from **1** to **5** can be proposed on account of the structures of the compounds and the time order of their

(12) (a) Luinstra G. A.; Teuben, J. H. *Organometallics* **1992**, *11*, 1793. (b) Beckhaus, R.; Thiele, K. H.; Ströhl, D. *J. Organomet. Chem.* **1989**, *369*, 43.

(13) Moore, J. W.; Pearson, R. G. *Kinetics and Mechanism*; John Wiley and Sons: New York, 1981; Chapter 8 (either on the reaction pathway to the final product or not).

(14) Bercaw, J. E.; Marvich, R. H.; Bell, L. G.; Brintzinger, H.-H. *J. Am. Chem. Soc.* **1972**, *94*, 1219.

appearance (depicted in Scheme 1). In the first step, the β hydrogen of the allyl in **1** is transferred to the fulvene, with formation of the allene adduct of permethyl titanocene **2**. In the next step, the activation of a C−H bond of a Cp* methyl group leads to the fulvene compound **3a**. In the sequence **1**−**3a**, the allyl fragment has been transformed into an isopropenyl group, corresponding to a net 1,2-hydrogen−titanium exchange [in the formalism of an η^1-allyl]. A hydrogen shift from the isopropenyl's methylene group gives the propyne adduct Cp^*_2-Ti(HC≡CMe) (**4**). We feel that the orientation of the 2-propenyl group in **3a** is such that a hydrogen may only be transferred to the fulvene unit from the methyl group, leading back to the allene complex **2**. For a productive process, the relative orientation of the fulvene and C_3-olefinic methylene groups has to change to a situation as in complex **3b**, where a close contact between the latter two is possible. Hence, the third step in the isomerization is a rotation around the Ti−C bond in **3a**, giving **3b**. The final product is derived from **4** through another hydrogen shift. The transformation of **3b** into **5** is likewise a net 1,2 hydrogen−titanium shift. This proposal is consistent with all observations.

There is, however, no a priori reason to assume that products are consecutively formed on going from **1** to **5** (Scheme 1) and that no reversible side reactions are taking place. It is, e.g., perfectly viable to propose a shunt between **2** and **4**, leaving **3a**,**b** in the middle as a kind of reservoir compound, not essential for the overall isomerization. We chose a mathematical approach to shed light on this matter and to find a set of rate constants to describe the concentration profiles of **1**−**5**, starting from either **1** or the mixture **3a**,**b**.

The Model and the Evaluation of the Rate Constants. Since all compounds in the isomerization have the same constitution, $C_{23}H_{34}Ti$, we will *presume* that rearrangements occur strictly intramolecularly and follow an exponential rate law. This assumption is justified by the observation that C−H activations in the closely related Cp^*_2TiR[15] and Cp^*_2TiRR' systems[11,16] (and Zr[17] and Hf[18]) all proceed intramolecularly. Isotope labeling experiments are not so useful here, since all steps are reversible, and scrambling of any deuterium label would soon take place. Selective carbon labeling would likewise give no additional information. It is further assumed that only reversible reactions occur between consecutively numbered compounds as in Scheme 1, leading to a tridiagonal matrix **K** containing the rate constants and specifying the set of coupled differential equations for dc_j/dt (see Appendix). Although an analytical solution exists for the occurring matrix−eigenvalue problem and thus for the differential equations describing a first-order reversible reaction system involving an arbitrary number of steps,[12] a numerical procedure was adopted to avoid practical problems[19] and to allow for an easy modification of the program to handle also alternative reaction schemes. The initial (or boundary) conditions are introduced as normalization factors for the eigenvectors of the **K** matrix. The difference between calculated and measured data was then minimized through a variation of the k_x values by a computer routine. Good fits were obtained in this manner. The final rate constants are given in Table 3 (see Experimental Section and Appendix). For sensitivity reasons, the first four rate constants k_1 to k_{-2} were most accurately obtained from the data starting from **1**, and k_3 to k_{-4} were most accurately obtained from the data of the isomerization starting from **3a**,**b**, since the respective concentrations are farthest away from the equilibrium and their changes are largest. A consistent value of k_5 was found for both data sets. Values for k_{-5} were calculated from the thermodynamic data of the equilibrium **4** ⇌ **5**. They are relatively small and contribute numerically only in a minor way, which leads to low accuracy if taken from the simulation. The values of k_1 to k_{-2} obtained from data starting from **3a**,**b** and the values of k_3 to k_{-4} obtained from data starting from **1** are within 30% of the tabulated numbers in Table 3 obtained from the other starting compounds. Thus, this demonstrates that the process is properly described by the sequence in Scheme 1.[20]

Table 3. Calculated Rate Constants of the Isomerization Process

	T (K)				
$k_{(-)x}$[a]	283.15	293.15	303.15	313.15	318.15
k_1	3.7×10^{-5}	1.5×10^{-4}	4.2×10^{-4}	1.2×10^{-3}	1.6×10^{-3}
k_{-1}	1.6×10^{-5}	5.8×10^{-5}	1.5×10^{-4}	3.7×10^{-4}	
k_2	7.1×10^{-5}	3.8×10^{-4}	1.2×10^{-3}	4.9×10^{-3}	
k_{-2}	2.7×10^{-5}	1.45×10^{-4}	4.6×10^{-4}	1.9×10^{-3}	
k_3	1.3×10^{-5}	5.3×10^{-5}	2.2×10^{-4}	5.4×10^{-4}	
k_{-3}	9.9×10^{-6}	3.5×10^{-5}	2.2×10^{-4}	4.5×10^{-4}	
k_4	8.4×10^{-5}	2.4×10^{-4}	1.6×10^{-3}	4.8×10^{-3}	
k_{-4}	9.6×10^{-6}	3.5×10^{-5}	2.6×10^{-4}	8.0×10^{-4}	
k_5	1.6×10^{-5}	4.3×10^{-5}	1.4×10^{-4}	3.5×10^{-4}	5.7×10^{-4}
k_{-5}	4.4×10^{-7}	1.3×10^{-6}	4.9×10^{-6}	1.4×10^{-5}	2.4×10^{-5}

[a] $k_{(-)x}$ in s^{-1}. k_1 through k_{-2} were obtained from measurements starting from **1**; k_3 through k_{-4} were obtained from data starting from the **3a**,**b** mixture. The numerical evaluation becomes insensitive in the course of the reaction when all compounds are present: concentrations and their changes are small. The ratios of k_x over k_{-x}, however, are found at the same values and are not dependent on starting conditions. Rate constant k_5 is consistently the same from both types of experiments. No reliable values for k_{-1} through k_{-4} could be obtained at 45 °C: the characterizing changes are too fast to measure by NMR methods.

Characteristics of the Isomerization Process. Data of the isomerization from **1** and from the mixture of **3a**,**b** were collected at four temperatures between 10 and 40 °C through time-dependent monitoring by ^{1}H NMR spectroscopy. Rate constants were subsequently determined with the aid of the procedure described above. The equilibrium constants and the activation energies for all equilibria were obtained from Eyring plots (Table 4). The observed good linearity of the Eyring plots, originating from fitting of four completely independent data sets, is a further indication for the reliability of the kinetical analysis. A schematic diagram of the potential surface of the isomerization at 300 K is given in Figure 3.

Although the experimental errors in the free energy of activation preclude a conclusive discussion, the qualitative outcome is in accordance with the experimental observations. Starting from **1**, it is apparent that the concentrations of **2** and **3a** will grow first, since the difference of the barrier from **3a** to **3b** is twice that of **1** to **2** and **2** to **3a**. Compound **3b** becomes detectable only in the later stages: it isomerizes with a small barrier to **4** and can exist only in its presence. Starting from the **3a**,**b** mixture, the sums of **3b** and **4** as well as of **3a** and **2** are constant for the first part of the thermolysis, consistent with

(15) Luinstra, G. A.; Teuben, J. H. *J. Am. Chem. Soc.* **1992**, *114*, 3361.
(16) McDade, C.; Green, J. C.; Bercaw, J. E. *Organometallics* **1982**, *1*, 1629.
(17) Schock, L. E.; Marks, T. J. *J. Am. Chem. Soc.* **1988**, *110*, 7701.
(18) Bulls, A. R.; Schaefer, W. P.; Serfas, M.; Bercaw, J. E. *Organometallics* **1987**, *6*, 1219.
(19) The analytical expression contains a sum of exponential terms. If the exponents differ largely in magnitude, the finite precision of a computer will easily lead to numerical inaccuracies in the evaluation of sums of this type. See also: Matsen, F. A.; Franklin, J. L. *J. Am. Chem. Soc.* **1950**, *72*, 3337. (b) McLaughin, E.; Rozett, R. W. *J. Chem. Educ.* **1972**, *49*, 482. (c) Wei, J.; Prater, C. D. *Adv. Catal.* **1962**, *13*, 203ff. Benson, S. W. *The Foundation of Kinetics* McGraw-Hill: New York, 1953.
(20) Exchange of the concentration of **3a** for that of **3b** in the model gave unrealistically high rate constants for k_4 and k_3 and a much poorer overall fit result.

Table 4. Eyring Activation (k_x, k_{-x}) and Thermodynamic Parameters (K) of the Isomerization of Cp*FvTi(η^3-C_3H_5) (**1**) to Cp*FvTiCH═CHMe (**5**)

transition		$\Delta Y_x^{\ddagger\,a}$	$\Delta Y_{-x}^{\ddagger\,a}$	ΔY^b
1 to **2**, $x = 1$	ΔH	78(3)	74(3)	7(2)
	ΔS	−51(12)	−73(12)	34(3)
	ΔG	93(7)	96(7)	−3(3)
2 to **3a**, $x = 2$	ΔH	100(4)	101(4)	−1(1)
	ΔS	30(15)	23(15)	6(2)
	ΔG	91(9)	93(9)	−3(2)
3a to **3b**, $x = 3$	ΔH	91(5)	96(10)	−5(5)
	ΔS	−17(17)	0(15)	−16(20)
	ΔG	96(10)	96(15)	∼0(11)
3b to **4**, $x = 4$	ΔH	102(9)	111(8)	−9(2)
	ΔS	35(31)	49(28)	−2(10)
	ΔG	91(18)	96(17)	−8(5)
4 to **5**, $x = 5$	ΔH	75(2)	84(2)	−9.1(3)
	ΔS	−72(5)	−70(5)	−2.0(1)
	ΔG	97(3)	105(3)	−8.5(4)
1 to **5**	ΔH			−17(6)[c]
	ΔS			+8(20)
	ΔG			−20(12)

[a] $\Delta Y_{(-)x}$ corresponds to enthalpies (ΔH, kJ/mol), entropies (ΔS, J/(mol·K)), and Gibbs energy (ΔG, kJ/mol, at 300 K) for transition x. [b] Equilibrium constants were calculated from $-RT \ln(k_x/k_{-x}) = \Delta G^0$. Errors in the kinetic and thermodynamic parameters were calculated on the basis of the linearity of the Eyring plots. The difference between two experimental data sets obtained at the same temperature is estimated to have a smaller impact on k_x than those otained from the fitting procedure. [c] From $-RT \ln(\prod k_x/\prod k_{-x}) = \Delta G^0$.

the higher barrier between **3a** and **3b** than that between **3a** and **2** or **3b** and **4**. Likewise, the concentration of **4** reaches a substantial level before the final product is formed, demonstrating the high free energy of activation for the last forward step. It is remarkable that the rotation **3a** to **3b** and vice versa has a higher barrier than some of the CH activation processes. There are no obvious reasons for this fact; it may reflect the steric congestion at the metal center: C−H activation proceeds with less steric interaction than rotation of the isopropenyl fragment past the methyl groups of Cp* and Fv ligands and, therefore, may have a lower Gibbs energy of activation.

A striking feature is that the Gibbs energies of activation at 300 K (Table 4) for the forward and reverse reactions are very similar, even though very different C−H bonds are involved. A couple of comparisons are made. The first concerns the transition between complexes **3a** and **3b**. The free activation energy for interconversion is the same in both directions. For the forward direction, however, the entropy contribution is much larger. This may reflect the fact that, in **3a**, two close contacts between fulvene methyl and C_3 ligand methylene are present, whereas, in **3b**, two methyl and two methylenes—of the fulvene and isopropenyl—are confined to the same space. The latter arrangement seems more hindered, giving **3b** apparently a smaller degree of freedom. Therefore, entropy is liberated toward the transition state to **3a**. This is in accordance with the tentatively assigned structures of **3a** and **3b**. Remarkable is that the formations of **2** from **1** and of **5** from **4** have negative activation entropies but, adversely, that the formation of **3a** from **2** and of **4** from **3b** have *positive* activation entropies. The same is found for the reverse of these reactions. This indicates that formation of (and transitions from) the sterically congested **3a**,**b** isomers proceeds through considerable bond stretching with concomitant liberation of entropy. This is the opposite of what is usually found for processes at formally d^0 complexes with tight transition states, characterized by negative activation entropies and small activation enthalpies with respect to bond energies and, indeed, is observed for the transitions not involving **3a**,**b**.[21] It is, however, unlikely that free radicals are formed, since activation enthalpies are still substantially below Ti−C bond dissociation energies.[22] It is, therefore, assumed that the hydrogen atom is transferred through the usual σ-bond metath-

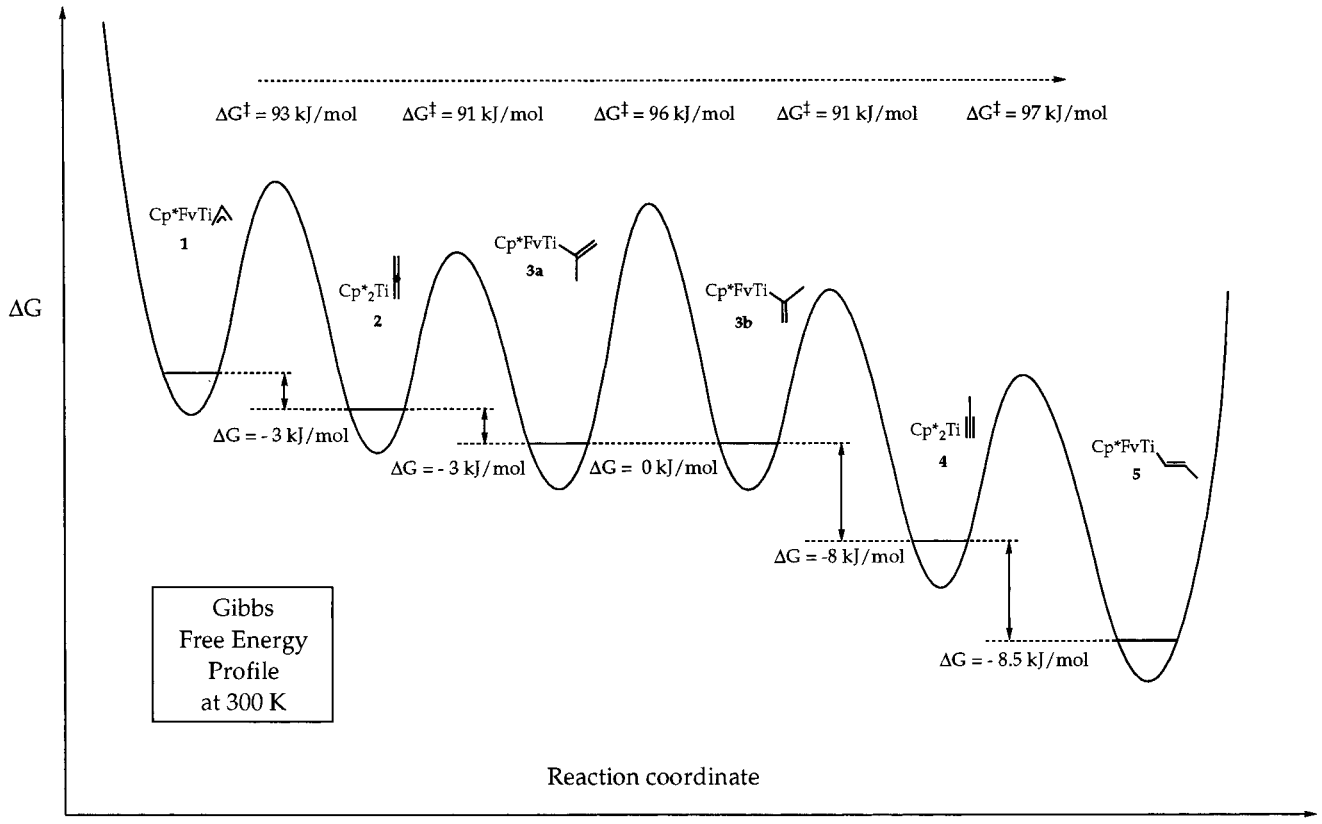

Figure 3. Gibbs free energy profile at 300 K for the isomerization of Cp*FvTi(allyl) (**1**) to Cp*FvTi-(*E*)-CH═CHMe (**5**).

esis between the involved entities. The positive activation entropies involving **3a**,**b** are explained by the sterically congested ground state, the strain being partly released toward the transition state.

The Gibbs free energy difference between **1** and **5** is 15 kJ/mol (at 300 K) and consists essentially of enthalpy. It may be concluded that this reflects the increasing Ti−C bond strength in Cp*FvTi vinyl vs allyl. From this, we can address the question of why the desired catalysis of L_nM−allyl to L_nM−vinyl is not operating. The thermodynamics of the system predicts that, for the transmetalation reaction to proceed, the Mg−allyl reagent must be at least 15 kJ/mol less stable than the (*E*)-Mg−propenyl to compensate for the difference in stability of **1** and **5**. Since the difference between the BrMg−allyl and −vinyl bond is −88 kJ/mol, this requirement is met, and kinetic barriers for transmetalation are likely to underlie the absence of catalysis.[23]

Concluding Remarks

In this paper, we describe the details of an isomerization reaction of an allyl to the specific orientation of a *trans*-1-propenyl fragment. The process proceeds on a very smooth energy surface with comparable stabilities for all intermediates and similar free energies of activation for all transitions.

Bercaw and coworkers[8] reported the isomerization of $Cp^*_2Ta(\eta^3\text{-}C_3H_5)$ to the exo isomer of $Cp^*_2TaH(=C=CHMe)$, which is proposed to proceed through the intermediate formation of tantalocene allene hydride $Cp^*_2TaH(H_2C=C=H_2)$ and $Cp^*_2TaCMe=CH_2$, which were not observed, and $Cp^*_2TaH(HC\equiv CMe)$, identified as the exo isomer. The mechanism for the formation of the final product, *exo*-$Cp^*_2TaH(=C=CHMe)$, from this propyne adduct is not obvious and is different from the Cp*FvTi system reported here. The formal oxidative addition of propyne is also unlikely in the Cp^*_2Ti system. The endo isomer of $Cp^*_2TaH(HC\equiv CMe)$ gives a 1-vinyl derivative ($Cp^*_2TaCH=CHMe$), from which the final product, *endo*-$Cp^*_2TaH(=C=CHMe)$, is formed by an α-H elimination.

It may thus be concluded that the C_3 fragment of the Cp*FvTi− and Cp^*_2Ta−allyl compounds undergoes isomerizations through very similar structures, the main difference being the position to which the hydride is moved. In the chemistry of $Cp^*_2Ta^{III}$, hydride olefin complex formation is thermodynamically favorable, whereas this is not so likely for Cp*FvTi. Intermediate hydrides, like Cp*FvTiH(allene) or Cp*FvTiH(propyne), would be appreciatively less stable due to the lack of back-bonding to the olefin (as for Ta(III)), and their formation prior to the appearance of allene or propyne adducts of titanocene derivatives is incompatible with the fact that **3b** gives **4** and **3a** gives **2** and vice versa. The propyne adduct is the most stable intermediate in both Ti and Ta compounds.

A general picture emerges from the observations in the Cp*FvTi system: *spatial* arrangements strongly determine the reaction modes for the CH activation reactions. The importance of relative orientations is especially manifested in the rotation around the Ti−C bond in the transition of **3a** to **3b**, which determines whether an allene or propyne adduct of Cp^*_2Ti is formed. The fulvene/Cp* hydrogen shuttle functions in that sense, similar to certain enzymes. These results indicate that fulvenes are formed in a concerted and direct way, i.e., without intermediate hydride formation. This is substantiated by the observation reported by Bercaw, that formation of Cp*FvTiH from Cp^*_2Ti proceeds only slowly.[24] In addition, no titanapentanes or -pentenes were detected—the products of a reaction between **2** or **4** with free allene or propyne.[25] The latter are expected to be liberated from **2** and **4** prior to or as a consequence of the formation of the d^0 compound Cp*FvTiH if this has taken place (vide supra).[26]

The reaction of **1** to **3a** can formally be considered to be an isomerization of a 1,2- to 2,1-inserted allene in the Ti−H bond of $Cp^*FvTi^{IV}H$ (and **3b** to **5** the same for propyne). In the actual mechanism of this reaction, β-hydrogen elimination is accompanied by a *formal reduction* of the metal center to $Cp^*_2Ti^{II}$, thus providing d electrons for stabilizing metal alkene (alkyne) adducts through back-donation. The unsaturated substrate thus never dissociates from the metal but still isomerizes. Such transformations may play a role in isomerization reactions in Ziegler−Natta polymerization, where olefin dissociation can be excluded as a reaction pathway.[27]

Acknowledgment. We thank Dr. A. Geyer and Ms. M. Cavegn for recording 2D spectra.

Appendix

Within the given model, the time dependence of the concentration $c_j(t)$ of compound j is described by

$$\frac{dc_j(t)}{dt} = k_{j-1}c_{j-1}(t) - (k_{-(j-1)} + k_j)c_j(t) + k_{-j}c_{j+1}(t) \quad (1)$$

where $j = 1...6$ and $k_x = 0$ if either $j - 1 < 1$ or $j + 1 > 5$. The corresponding set of coupled differential equations can be written in matrix form as

$$\dot{\mathbf{c}}(t) = \mathbf{K}\mathbf{c}(t) \quad (2)$$

where **K** is the (in this case tridiagonal) matrix containing the rate constants, while $\dot{\mathbf{c}}(t)$ and $\mathbf{c}(t)$ are the vectors containing (in row j) $dc_j(t)/dt$ and $c_j(t)$, respectively. For the solution of a set of consecutive first-order reactions, one can use the ansatz

$$\mathbf{c}(t) = \sum_{n=1}^{6} e^{\lambda_n t}\mathbf{x}_n \quad (3)$$

leading to

$$\dot{\mathbf{c}}(t) = \sum_{n=1}^{6} \lambda_n e^{\lambda_n t}\mathbf{x}_n \quad (4)$$

Inserting eqs 3 and 4 into eq 2 yields the eigenvalue problem

$$\sum_{n=1}^{6} (\mathbf{K} - \lambda_n\mathbf{E})\mathbf{x}_n = 0 \quad (5)$$

where **E** is the unity matrix. The solution of the eigenvalue

(21) Thompson, M. E.; Baxter, M. S.; Bulls, R.; Burger, B. J.; Nolan, M. C.; Santarsiero, B. D.; Schaefer, W. P.; Bercaw, J. E. *J. Am. Chem. Soc.* **1987**, *109*, 203.

(22) Martinho Simoes, J. A.; Beauchamp, J. L. *Chem. Rev.* **1990**, *90*, 629 and references therein.

(23) Holm, T. *J. Chem. Soc., Perkin Trans. 2* **1981**, *2*, 464.

(24) Bercaw, J. E. *J. Am. Chem. Soc.* **1974**, *96*, 5087.

(25) Cohen, S. A.; Bercaw, J. E. *Organometallics* **1985**, *4*, 1006.

(26) This likewise explains why Cp^*_2TiH is so much less stable than Cp^*_2TiMe toward decomposition to Cp*FvTi: a hydrogen s orbital more readily accepts a hydrogen than an sp^3-hydridized carbon; see ref 16.

(27) Leclerc, M. K.; Brintzinger H.-H. *J. Am. Chem. Soc.* **1996**, *118*, 9024.

problem given in eq 5, i.e., the eigenvalues λ_n and the non-normalized eigenvectors $\mathbf{x}_n$, is usually (and also in this work) obtained by a diagonalization of the **K** matrix.

The remaining problem is the evaluation of the normalization factors of the eigenvectors $\mathbf{x}_n$. The normalization factors can already be obtained if all concentrations are exactly known at a single time value. Since it was experimentally possible to start from the pure compound **1**, the normalization factors can readily be obtained from the corresponding initial condition $c_1(t = 0) = 1$ and $c_{j=2...6}(t = 0) = 0$. When starting from **1**, one finds, therefore, for the vector **N** containing the normalization factors, the relation $\mathbf{N} = \mathbf{X}^{-1}\mathbf{c}(t = 0)$, where the *i*th column of matrix **X** contains the eigenvector $\mathbf{x}_i$.

However, when starting from the mixture **3a**,**b**, a more difficult situation is encountered, since, in that case, the initial condition is not exactly defined. Of course, it would still be possible to use the concentrations at one time value for determining the normalization factors, but these factors would depend on the accuracy of the measured concentrations at only a single time value. To decrease the dependence on incidental experimental errors, an alternative procedure for determining the normalization factors was adopted, i.e., all experimental data were used to define the boundary conditions for the differential equations. The advantage of such a procedure is that the accuracy of the evaluation of the normalization factors relies on all available data points, and thus one can expect a partial cancelation of errors in individual data points. The vector **N** is now obtained from

$$\mathrm{N} = \begin{bmatrix} \mathbf{x}_1 e^{\lambda_1 t_1} & \mathbf{x}_2 e^{\lambda_2 t_1} & \cdots & \mathbf{x}_6 e^{\lambda_6 t_1} \\ \mathbf{x}_1 e^{\lambda_1 t_2} & \mathbf{x}_2 e^{\lambda_2 t_2} & \cdots & \mathbf{x}_6 e^{\lambda_6 t_2} \\ \mathbf{x}_1 e^{\lambda_1 t_3} & \mathbf{x}_2 e^{\lambda_2 t_3} & \cdots & \mathbf{x}_6 e^{\lambda_6 t_3} \\ & \cdots & & \end{bmatrix}^{-1} \begin{bmatrix} \mathbf{c}(t_1) \\ \mathbf{c}(t_2) \\ \mathbf{c}(t_3) \\ \cdots \end{bmatrix} \tag{6}$$

In both cases (initial or boundary condition), the inverse matrices were evaluated by a singular-value decomposition (corresponding to a linear least-squares solution).

For a given set of rate constants, the concentrations $c_j^{\mathrm{calc}}(t)$ are finally calculated according to

$$\mathbf{c}^{\mathrm{calc}}(t) = \sum_{n=1}^{6} N_n e^{\lambda_n t} \mathbf{x}_n \tag{7}$$

The quantity

$$\chi^2 = \sum_i \sum_j \frac{[c_j^{\mathrm{exp}}(t_i) - c_j^{\mathrm{calc}}(t_i)]^2}{|c_j^{\mathrm{exp}}(t_i)|} \tag{8}$$

was then minimized by restricting k_x to real and positive values.

Supporting Information Available: Representative examples of the experimental data with fitted curves for the isomerization of **1** at 20 °C and of **3a**,**b** at 10 and 40 °C and Eyring plots of the temperature dependence of the rate constants (19 pages). See any current masthead page for ordering information and Web access instructions. The FORTRAN code may be obtained from A.S.

JA972867B